# Detecting biomolecules with nanoscale active electronic devices.

G. Gruner
Nanomix Inc.
Emeryville CA 94508
and
Department of Physics
University of California Los Angeles
Los Angeles, CA 90095

## ABSTRACT

Nanoscale electronic devices offer bio-detection schemes that are complementary to optical detection methods. This paper reviews the utilization of field effect transistor devices with carbon nanotubes as conducting channels –the device architectures and detection schemes are reviewed in the paper 5592-34 presented at this meeting– for the detection and monitoring biological processes such as ligand-receptor interactions and enzymatic processes. A complex device with both biological and electronic functionality is also discussed.

## 1. INTRODUCTION

Because of the rich potential of biosensors[1] and bioelectronics,[2] recent research has focused on the interactions between biomolecules and inorganic systems. The integration of biological processes and molecules with fabricated structures also offers both electronic control and sensing of biological systems and biologically electronic driven nanoassembly[3]. As a specific example, carbon nanotubes have been suggested for use as prosthetic implants in nervous systems[4], this goal requires the integration of fully functioning biological and nanoelectronic systems. Thus far, researchers have used organic and inorganic chemistry to attach proteins[5], DNA[6], and lipids[7] to nanotubes, nanowires, and nanocrystals. In such bottom-up construction, a single biological species is integrated with a single type of nanostructure, usually in solution. To move towards functional devices, further processing is required, which may damage the biological molecules. Alternatively, to make more complex biological structures requires that biological activity be preserved despite the presence of the nanostructures. As a result, the nanostructures have served only as mechanical supports, without electronic functionality[2].

Nanotubes have been functionalized to be biocompatible and to be capable of recognizing proteins.[8-11] Often, this functionalization has involved non-covalent binding between a bi-functional molecule and a nanotube to anchor a bio-receptor molecule with a high degree of control and specificity. The unique geometry of nanotubes has also been used to modify nanotube-protein binding. The conformational compatibility, driven by both steric and hydrophobic effects, between proteins and carbon nanotubes has been examined using streptavidin and other proteins. For example, streptavidin has been crystallized in a helical conformation around multiwalled carbon nanotubes.[12] Conversely, the tendency of biological materials to self-organize has been used to direct the assembly of nanotube structures.[13]

In the paper 5592-34, presented at this meeting the operation and environmental response of the of various transistor geometries is discussed together with issues pertaining the interaction of the devices with biomolecules. The examples that that will be discussed here demonstrate the power of electronic detection methods in revealing certain important aspects of biological reactions, and the bio-electronic interface.



Nanosensing: Materials and Devices, edited by M. Saif Islam, Achyut K. Dutta,
Proceedings of SPIE Vol. 5593 (SPIE, Bellingham, WA, 2004)
0277-786X/04/$15 · doi: 10.1117/12.570824

## 2. SENSING BIOLOGICAL PROCESSES USING NANOTUBE FET DEVICES.

The examples given in 5592-34 illustrate the interaction between the bio-molecules and the electronic devices. The experiments summarized there give important insight into biomolecule immobilization issues, but also lay the ground work for electronic detection of biological processes. Two examples, that take the electronic detection of biological reaction concept one step further are given here: the detection of ligand-receptor binding and the detection of an enzymatic reaction.

### 2.1.Ligand-receptor interactions

Monitoring specific interactions between biomolecules remains one of he most important objectives of biosensing[14-16]. The detection scheme that involves electronic detection is shown in **Figure 1a**. First a polymer layer is applied to the device in order to avoid nonspecific biomolecule binding. Subsequently a ligand is attached to the layer, such ligand serves as the recognition site through ligand-receptor binding. Finally, the resulting structure is incubated with the receptor in order to explore the binding process. All these steps can readily be followed by examining the device characteristics after each step. The scheme is expected to work for a broad variety of interactions, and may be appropriate even for detecting DNA duplex formation. In Ref. 14, PEI/PEG layer, biotin as the ligand and gold labeled streptavidin as the receptor was used. We have found that the PEI/PEI layer effectively prevents (in contrast to what we have found in non-functionalized nanotubes) the binding of streptavidin to the device. After polymer coating, biotin was covalently attached to the polymer and the device was subsequently incubated with gold nanoparticle-labeled streptavidin. The SEM image, shown in **Figure 1b** is the realization of the architecture, and of the end-result of the incubation process. The image clearly identifies the gold particles along the nanotube, giving evidence of streptavidin binding onto the nanotube in question. With a length of 800nm of the nanotube, and a gold sphere diameter of 10nm, it is expected that, upon full coating there are approximately 80 streptavidin molecules in direct interaction with the nanotube conducting channel, in good agreement with what one concludes through direct examination of the image. Biotin-streptavidin binding has been detected by changes in the device characteristic. The resulting change of the DC is displayed in **Fig.2a**. Instead of the shift of the DC one observes a suppression of the conduction, most likely due to some distortion of the nanotube, caused by the presence of streptavidin, such distortion leading to a carrier scattering, and thus reducing the mobility of the channel. The change exceeds the noise limit by a factor of approximately 10, leading to the conclusion that the current detection limit is about 10 proteins. Various control experiments have also been conducted. Non-specific binding was electronically detected in case of streptavidin (**Figure 6** in 5592-34) before, but - as discussed above - a PEI/PEG layer was found to prevent nonspecific binding, and indeed no change of the device characteristic was found

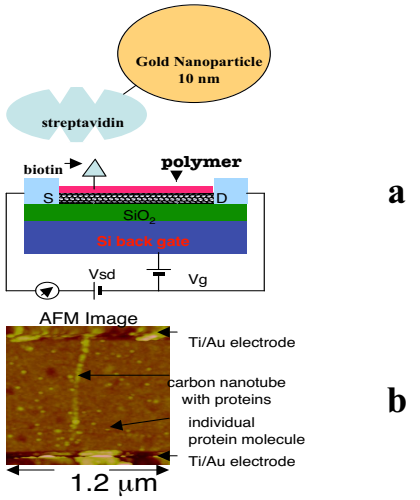


Fig.1. a) Detection scheme for biotin-streptavidin ligand receptor binding. b) AFM image of the device after incubation with gold labeled streptavidin. The vertical line with bright dots is the nanotube channel indicating streptavidin attachment, mainly to the nanotube.

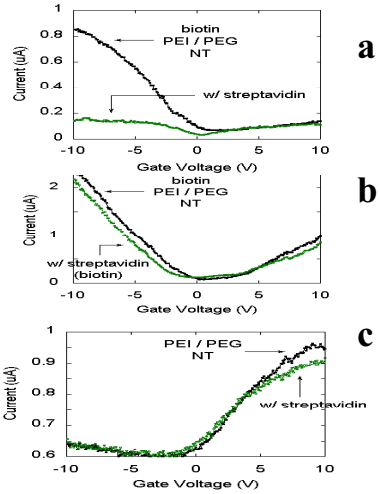


Fig 2. Ligand receptor binding between biotin and streptavidin. a) response of device illustrated on fig 1a. b) control experiment involving biotinilated streptavidin. c) control experiment using the device illustrated in Fig 1a, but without biotin attachment.

when polymer-coated devices were incubated with streptavidin and other proteins (**Figure 2c**). Control experiments involving biotinilated streptavidin with the binding sites already occupied by biotin did not, as expected, result in binding. This is indicated by the fact that the device characteristics did not change upon incubation (**Figure 2b**).

### 2.2. Enzymatic reactions

As an example of the application of devices for the electronic monitoring of an enzymatic reaction[17-19], the enzymatic hydrolysis of starch has been performed[20]. Starch consists of linear component, amylose which is composed of linkages between D-glucopyranose residues, and amylopectin, the branched one, which in addition to a-1,4 linked D-glucopyranose chains carry branches at C-6 on every 25 or so D-glucopyranose residues which also have the a-configuration [21]. We have characterized starch enzymatic hydrolysis with amyloglucosidase [22] in acidic buffer, resulting in complete cleavage of the polymer to water soluble glucose. Enzymatic hydrolysis of starch using amyloglucosidase in solution has been shown to be efficient in precipitating carbon nanotubes from their solution.

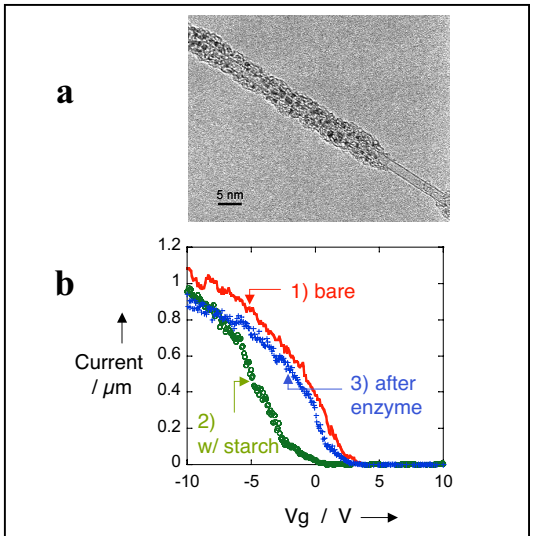


Fig.3. Enzymatic degradation of starch a) starch coated nanotube, b) device characteristics before, and after starch deposition and after the enzymatic degradation of starch.

The starch covered single wall nanotubes (SWNT) were studied by transmission electron microscopies. **Figure 3a** shows high-resolution electron transmission (HRTEM) image of SWNT covered with starch. For imaging purposes, the starch was contrasted by using $RuO_4$ staining procedure. After starch deposition, the DC shifts by approximately ~ 2 volts toward negative gate voltages (**Figure 3b**) corresponding to electron doping of the nanotube channel by polymer. Compared to other polymers, such as poly(ethylene imine) (PEI), the magnitude of the shift is small. This fact, most likely, relates to difference between electron donating ability of alcohol and ether groups in starch as compare to amines in PEI. After the enzymatic reaction was completed on the starch functionalized device, the device response observed before starch deposition (**Figure 3b**) is recovered, indicating that during enzymatic reaction all the starch is hydrolized to glucose, with the hydrolization product washed off prior to the electronic measurements. Two control experiments were performed to confirm these results. First, the starch functionalized chip was rinsed with buffer to see if the buffer alone can wash away the starch deposited on the device. The DC after rinsing with buffer solution is similar to that obtained before rinsing, leading to the conclusion that starch removal by buffer alone does not occur. Another control experiment involved the deposition of enzyme solution on bare devices. The DC shows increased hysteresis but no significant shifting has been observed – giving evidence that enzyme alone does not lead to charge transfer.

## 3. BIO-ELECTRONIC INTEGRATION: BACTERIORHODOPSIN, BR IN A PURPLE LAYER

The next example involves a bio-entity with well defined biological function – a protein-membrane compex[23]. As the cell membrane, we have chosen the purple membrane (PM) from *Halobacterium salinarum*[24], which has been widely studied. PM contains the light-sensitive membrane protein bacteriorhodopsin, which serves as a photochemical proton pump and has been used to fabricate phototransistors. The structure is depicted in **Figure 4a**. In addition, rhodopsin has a permanent electric dipole moment, a charge distribution which produces an electric field pointing from the extracellular side of the membrane towards the cytoplasmic side[23]. These properties make PM an ideal prototype membrane for nanobioelectronic integration. In particular, we use the dipole as an indicator that the integration preserves the biomaterial while bringing it into contact with the nanoelectronic devices.

PM isolated from *Halobacterium salinarum*[24] was deposited on devices. To observe the effect of the electric dipoles fixed in the PM, devices were prepared in three conditions, as shown in **Fig. 4b**: with the cytoplasmic side of the PM facing the nanotubes[25], with the extracellular side facing the nanotubes[25], and with a mixture of both orientations[26]. The particular orientation was achieved by applying a gate voltage as described in **Fig 4** of +3V or –3V. Such voltage leads to electric field oriented according to the voltage polarity at the nanotube network surface. Such changes by interacting with the electric dipoles of the bR in the purple membrane are most likely responsible for the gate voltage influenced deposition.

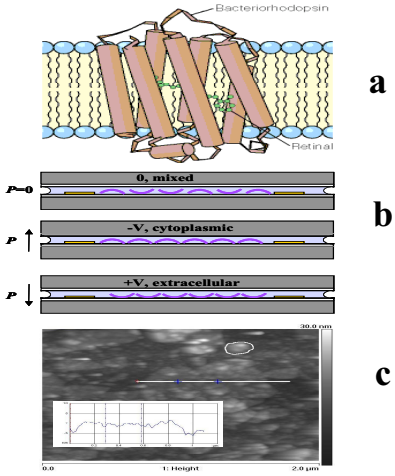


Fig 4. a). Illustration of bacteriorhodopsin in a purple membrane. b). Three purple membrane, PM arrangements, random, cytoplasmic and extracellular, deposited by employing 0, -3V and +3V voltages. The grey areas correspond to two Si chips, and the voltages were applied between the two chips. The voltages listed correspond to the potential on the top chip. c). AFM image of deposited PM, the scan indicates the height of the membrane, approximately 5nm.

The structure we have examined is a dense network of individual carbon nanotubes (**Fig. 2 of 5592-34**) covered by the membrane, referred to as a nanotube network field-effect transistor (NTN-FET). The deposition of purple membrane has been examined by AFM imaging, such image is shown in **Fig. 4c**. One observes layers of 5nm height, corresponding to a single layer of the membrane. This configuration has several significant features. First, the cell membrane is in direct contact with the semiconducting channel of the transistor. This is distinct from previous work, in which cell membranes have contacted the gate electrodes of transistors[23]. In this configuration, transistors detect the electrical potential across membranes; in contrast, our devices detect local electrostatic charges on the biomolecules. Second, the use of a large number of nanotubes ensures that entire patches of membrane are in contact with nanotubes.

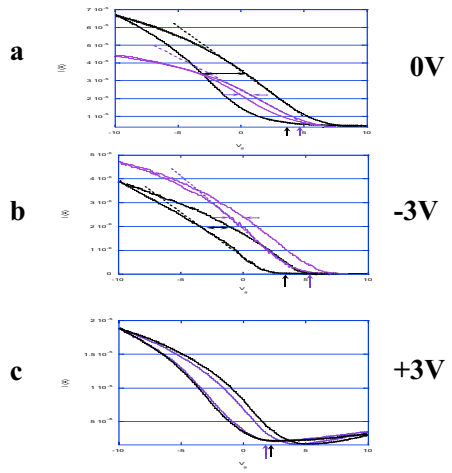


Fig. 5. a) Device characteristics for a device before (black) and after (purple) the deposition of cell membrane. Each DC has two curves, from the right-moving sweep of gate voltage and the left-moving. The intrinsic threshold voltage, indicated by black and purple arrows respectively, is the average between the two sweeps.
b) DC before (black) and after (purple) the deposition of membrane oriented with the cytoplasmic side contacting the nanotubes.
c) DC before (black) and after (purple) the deposition of membrane oriented with the extracellular side contacting the nanotubes.

**Figure 5a** highlights three main device parameters before and after deposition for a typical device without the application of a voltage (resulting in a randomly oriented membrane). The changes were observed repeatedly in several devices prepared in the same way. First, the hysteresis loops narrowed significantly, as indicated by the arrows. Second, the threshold voltage changed by +1.0 ± 0.2 V, as indicated by the arrows on the x-axis. Finally, the device characteristics decreased by about 20% for negative gate voltages. These changes show that the PM has been successfully integrated with the NTN-FETs.

Next, we compare the effects of oriented PM deposition. In both orientations **(Figs. 5b and 5c)** the membrane deposition caused a narrowing of the hysteresis loops similar to that caused by the mixed-orientation deposition. At the same time, the threshold voltages shifted, in opposite directions according to the orientation of the membrane. Finally, the transconductance did not change, although the maximum conductance changed in accordance with the shifts in the threshold voltage.

First, we discuss the change of the device characteristic upon deposition of a randomly oriented membrane. This quantity is associated with the capacitance between the nanotube network, which forms the channel, and the gate; and with the mobility of carriers within the nanotube network. The capacitance is unlikely to

change as a result of membrane deposition; and this is confirmed by the fact that the transconductance is not changed by oriented membrane deposition. In the case of mixed-oriented membrane deposition, the alternation of positive and negative electric dipoles on a length scale of about 500 nm (the diameter of a typical patch of PM) should act as a significant random scattering potential, which decreases the carrier mobility in the network[27]. Thus, the decrease in DC in **Fig. 5a** is a direct result of the mixture of orientations. Second, the hysteresis decreased dramatically in all cases as a result of the biological coating. The hysteresis is known to result from adsorbed water on the substrate[28]; in addition, coatings which displace water from the nanotubes reduce the hysteresis. Consequently, we expect a decrease in hysteresis here as well, presuming that the PM remains intact as a layer contacting the nanotubes. Moreover, the width of the remaining hysteresis is similar for all three conditions, which suggests that the amount of PM coverage is similar. This conclusion was confirmed in randomly selected spots that were imaged by AFM. Third, the shift of the threshold voltage in the devices results from the electrostatic field associated with the bacteriorhodopsin electric dipole. This field induces charge in the nanotubes, thus shifting the Fermi level[29]. The position of the Fermi level is measured by the threshold voltage, and prior work has established the relationship between the threshold voltage in various device configurations and the quantity of charge induced in the nanotubes[30-32]. Using these works, we have evaluated the shift caused by mixed-orientation PM deposition and find an induced charge of 16 aC/mm of nanotube length.

Several important conclusions can be reached. First, the electronic device functionality is preserved. Second, the PM remains intact as a layer, and the bacteriorhodopsin membrane proteins retain their electric dipoles. Third, the deposited PM has been demonstrated to contact the device directly and to interact with it's electrical properties.

One can also examine the significant asymmetry between cytoplasmic and extracellular orientations. This asymmetry is reflected in the large amount of charge induced in mixed-orientation devices, since without an asymmetry, the charge induced by equal amounts of cytoplasmic- and extracellular-oriented PM should cancel[33]. Such an asymmetry is known to exist, in that the dipole is closer to one side of the PM than the other[34]. Here we are able to observe this asymmetry directly because of the device configuration in which the PM contacts the nanotubes directly. One can quantify the asymmetry, by modeling the electrostatic effect of the bacteriorhodopsin dipole on the nanotubes[31] and the model is depicted in **Fig.6** Furthermore, we can quantify the asymmetry, by modeling the electrostatic effect of the bacteriorhodopsin dipole on the nanotubes[35]. The dipole is still not well understood, but it is known to result from the competition between several charge distributions that result in a net dipole moment of $3.3\times10^{-28}$ C·m per rhodopsin monomer. To calculate the effect of this dipole on the nanotubes, we use a simple electrostatic model in which the rhodopsin molecules above a nanotube (**Fig. 6**) form a line of constant dipole density. In this model, the line of dipoles with a density $\pi$ induces a charge density, $\lambda$, given by $\lambda = -r\pi/d^2$. Thus, by combining the known dipole moment of bacteriorhodopsin with the induced charge (measured from the threshold voltage shift and the known capacitance), we calculate how far the dipoles lie from the nanotubes. The answer will be different for the two different orientations, reflecting the position of the dipoles closer to one side of the PM. For the cytoplasmic orientation, with $\Delta V_{cp} = +2.2$ V, $d_{cp} = 1.9$ nm. For the extracellular orientation, with $\Delta V_{ec} = -0.4$ V, $d_{ec} = 4.4$ nm. Since the sum of these distances, 6.3 nm, is comparable to the membrane bilayer thickness of 5 nm[34], we conclude that this simple model is reasonable. Note, in particular, that since the ratio between $\Delta V_{cp}$ and $\Delta V_{ec}$ is 5.5, the electrostatic model indicates that $d_{cp}$ is 2.3 times smaller than $d_{ec}$. Thus, our data contribute additional details about the asymmetry of the bacteriorhodopsin charge distribution.

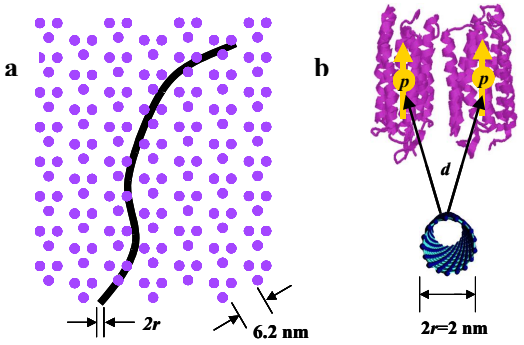


Fig 6. a. Model illustrating the geometry of PM with respect to the nanotubes. Rhodopsin (purple dots) assembles into trimers, which are arranged on a hexagonal lattice. The nanotube is a curved line. b. Model illustrating the dimensions used in the calculations. A rhodopsin monomer situated near a nanotube has a dipole moment p. This point dipole is situated within the rhodopsin at a distance d from the nanotube surface.

## 4. CONCLUSIONS

In conclusion, enough is now known about nanoelectronics that we are able to use a nanodevice as an investigative tool. One can use these devices for monitoring a variety of biologically significant reactions. This is possible because most of such reactions involve local electric fields and also charge rearrangement. We have also used the interaction between a biological system and a nanodevice not to learn about the electronic component, but to learn about the biological component. As a result, it should be possible to connect living cells directly to these nanoelectronic devices. The stage is set for the next phase of nanotechnology research.

The above concepts could conceivably be extended at a later stage to include of what one could call "cellectronics,,, cell-based electronic sensing: measuring the electronic response of living systems, and to using nanoscale devices for in-vivo applications: studying cell physiology, medical screening and diagnosis. The sensor architectures can be turned into devices where – by applying a voltage between elements of the sensor – surface charges can be created on the sensing element where the bio-molecules are immobilized. Such surface charges will interact with the charged bio-molecules, but such, potentially important effects have not been explored to date. The small size of the nanotube devices also allows the integration of the devices into living organisms. This will allow in-vivo electronic detection of biological processes.

## ACKNOWLEDGEMENTS

The experiments reported here were performed by K. Bradley, A. Star, J.C. Gabriel and A. Davis. They also contributed to the development of concepts in the area of nano-bioelectronic interface. This work was also supported by the NSF grant, 0415130.

## REFERENCES


1. M. Robers. I.J.A.M. Rensink, C.E. Hack, L.A. Aarden, C.P.M. Reutelingsperger, J.F.C. Glatz and W.T. Hermens , "A new principle for rapid immunoassay of proteins based on in situ precipitate-enhanced ellipsometry,,. Biophysical Journal. **76**, pp 2769-2776 (1999)
2. C.J, McNeil, D. Athey, On Ho Wah, "Direct electron transfer bioelectronic interfaces: application to clinical analysis,,, Biosensors & Bioelectronics **10**, pp.75-83 (1995)
3. I. Willner, "BIOELECTRONICS: Biomaterials for Sensors, Fuel Cells, and Circuitry,,, Science **298**, 2407 (2002).
4. H. Hu, Y. Ni, V. Montana, R. C. Haddon, V. Parpura, "Chemically Functionalized Carbon Nanotubes as Substrates for Neuronal Growth,,, Nano Letters **4**, 507 (2004).
5. D. Pantarotto, C. D. Partidos, R. Graff, J. Hoebeke, J.-P. Briand, M. Prato, A. Bianco, "Synthesis, Structural Characterization, and Immunological Properties of Carbon Nanotubes Functionalized with Peptides,,, J. Am. Chem. Soc. **125**, 6160 (2003).
6. Ming Zheng, Anand Jagota, Michael S. Strano, Adelina P. Santos, Paul Barone, S. Grace Chou, Bruce A. Diner, Mildred S. Dresselhaus, Robert S. Mclean, G. Bibiana Onoa, Georgii G. Samsonidze, Ellen D. Semke, Monica Usrey, and Dennis J. Walls, "Structure-Based Carbon Nanotube Sorting by Sequence-Dependent DNA Assembly,,, Science **302**, 1545 (2003).
7. Cyrille Richard, Fabrice Balavoine, Patrick Schultz, Thomas W. Ebbesen, and Charles Mioskowski, "Supramolecular Self-Assembly of Lipid Derivatives on Carbon Nanotubes,,, Science **300**, pp 775-778 (2003).
8. M. Shim, N. W. Shi Kam, R. J. Chen, Y. Li, H. Dai, "Functionalization of Carbon Nanotubes for Biocompatibility and Biomolecular Recognition,,, Nano Lett. **2**, pp 285-288 (2002)
9. W. Huang, S. Taylor, K. Fu, Y. Lin, D. Zhang, T. W. Hanks, A. M. Rao, Y.-P. Sun, "Attaching Proteins to Carbon Nanotubes via Diimide-Activated Amidation,,, Nano Lett. **2**, pp 311-314 (2002)
10. R. J. Chen, Y. Zhang, D. Wang, H. Dai, "Noncovalent Sidewall Functionalization of Single-Walled Carbon Nanotubes for Protein Immobilization,,, J. Am. Chem. Soc. **123**, pp 3838-3839 (2001)
11. Jason J. Davis, Malcolm L. H. Green, H. Allen O. Hill, Yun C. Leung, Peter J. Sadler, Jeremy Sloan, Antonio V. Xavier and Shik Chi Tsang, "The immobilisation of proteins in carbon nanotubes,,, Inorganica Chimica Acta **272**, pp 261-266 (1998)
12. F. Balavoine, P. Schultz, C. Richard, V. Mallouh, T.W. Ebbesen, C. Mioskowski, "Helical crystallization of proteins on carbon nanotubes: A first step towards the development of new biosensors,,, Angew. Chem. Int. Ed. **38**, pp 1912-1915. (1999)
13. G. R. Dieckmann, A. B. Dalton, P. A. Johnson, J. Razal, J. Chen, G. M. Giordano, E. Munoz, I. H. Musselman, R. H. Baughman, R. K. Draper, "Controlled Assembly of Carbon Nanotubes by Designed Amphiphilic Peptide Helices,,, J. Am. Chem. Soc. **125**, pp 1770-1777 (2003)
14. A. Star, J.-C.P. Gabriel, K. Bradley, G. Gruner, "Electronic Detection of Specific Protein Binding Using Nanotube FET Devices ,,, Nano Lett. **3**, pp 459-463 (2003)
15. R.J. Chen, S. Bangsaruntip, K.A. Drouvalakis, N. Wong Shi Kam, M. Shim, Y. Li, W. Kim, P. J Utz,. H. Dai, "Noncovalent functionalization of carbon nanotubes for highly specific electronic biosensors,,, Proc. Natl. Acad. Sci. USA **100**, pp 4984-4989 (2003)
16. K. Besteman, J.-O. Lee, F.G.M. Wiertz, H.A. Heering, C. Dekker, "Enzyme-Coated Carbon Nanotubes as Single-Molecule Biosensors,,, Nano Lett. **3**, pp 727-730 (2003)
17. W. Schnabel, *Polymer Degradation,* Chapter 6, Henser International: Berlin, 1981.
18. R. P. Wool, D. Raghavan, G. C. Wagner, S. J. Billieux, "Biodegradation Dynamics of Polymer-Starch Composites,,, Appl. Polym. Sci. **77**, pp 1643-1657 (2000)
19. M. V. Moreno-Chulim, F. Barahona-Perez, G. Canche-Escamilla, "Biodegradation of starch and acrylic-grafted starch by Aspergillus niger,,, Appl. Polym. Sci. **89**, pp 2764-2770 (2003)
20. A. Star, V. Joshi, T.-R. Han, M. V. P. Altoe, G. Gruner, J. F.Stoddart,, "Electronic Detection of the Enzymatic Degradation of Starch ,,, Org. Lett. **6**, pp 2089-2092 (2004)
21. P. Collins, R. Ferrier, *Polysaccharides: Their Chemistry*, pp. 478-523, John Wiley & Sons, Chichester, 1995 (b) J. Lehmann, *Carbohydrates: Structure and Biology*, pp. 98-103, Georg Thieme Verlag, Stuttgart, 1998 (c) D.B. Thompson, "On the non-random nature of amylopectin branching", Carbohydr. Polym. **43**, pp 223-239 (2000)
22. T. Yamamoto, *Enzyme Chemistry and Molecular Biology of Amylases and Related Enzymes*, pp. 3-201, CRC press, Inc. 1995,

23. K. Bradley, A. Davis, J-C. P. Gabriel and G. Gruner, " Nanobioelectronics: integration of cell membranes and nanotube transistors (to be published)
24. D. Oesterhelt, and W., Stoeckenius, "Functions of a New Photoreceptor Membrane „, Proc. Natl. Acad. Sci. U.S.A. **70**, pp 2853-2857 (1973)..
H.J. Steinhoff, R. Mollaaghababa, C. Altenbach, K. Hideg, M. Krebs, H.G. Khorana, W.L. Hubbell, "Time-resolved detection of structural changes during the photocycle of spin-labeled bacteriorhodopsin„, Science **266**, pp 105-107 (1994).
25. G. Vaŕo, Acta Biol. Acad. Sci. Hung. **32**, 301 (1981)..
26. . Yi Shen, Cyrus R. Safinya, Keng S. Liang, A. F. Ruppert, Kenneth J. Rothschild, "Stabilization of the membrane protein bacteriorhodopsin to 140 °C in two-dimensional films„, Nature **366**, pp 48-50 (1993).
K. Koyama, N. Yamaguchi, and T. Miyasaka, "Antibody-mediated bacteriorhodopsin orientation for molecular device architectures„, Science **265**, pp 762-765 (1994)
27. . Sander J. Tans, Cees Dekker, "Molecular transistors: Potential modulations along carbon nanotubes „, Nature **404**, pp 834-835 (2000).
28. K. Bradley, J. Cumings, A. Star, J.-C. P. Gabriel, G. Gruner, "Influence of Mobile Ions on Nanotube Based FET Devices„, Nano Lett. **3**, pp 639-641 (2003)
29. M. Freitag, M. Radosavljevic, Y. Zhou, A. T. Johnson, W. F. Smith, "Controlled creation of a carbon nanotube diode by a scanned gate„, App. Phys. Lett. **79**, pp 3326-3328 (2001).
30. Marc Bockrath, David H. Cobden, Paul L. McEuen, Nasreen G. Chopra, A. Zettl, Andreas Thess, and R. E. Smalley, "Single-Electron Transport in Ropes of Carbon Nanotubes„, Science **275**, pp1922-1925 (1997).
31. Ali Javey, Hyoungsub Kim, Markus Brink, Qian Wang, Ant Ural, Jing Guo, Paul McIntyre, Paul McEuen, Mark Lundstrom, Hongjie Dai, "High- dielectrics for advanced carbon-nanotube transistors and logic gates„ Nature Mat. **1**, pp 241-246 (2002).
32. K. Bradley, J-C P. Gabriel, M. Briman, A. Star, and G. Gruner, "Charge Transfer from Ammonia Physisorbed on Nanotubes „, Phys. Rev. Lett. **91**, pp 218301 (2003).
33. This assumption, that the mixed-orientation film contains equal amounts of cytoplasmic and extracellular orientations, is justified by our AFM images.
34. B. Ehrenberg, and Y. Berezin, "Surface potential on purple membranes and its sidedness studied by a resonance Raman dye probe, Biophys. J., **45**, pp 663-670 (1984)
35. The background charge due to the phosphate heads of the lipids is 0.2 electrons per square nanometer (24), which is too weak to explain the charge induced in our devices.